The Kinetics of Transformation in Zn-Al Superplastic Alloys

FU-WEN LING AND DAVID E. LAUGHLIN

We report herein on the kinetics of transformation of a eutectoid Zn-Al alloy containing additions of Cu, Mg and Ca. The alloy possesses excellent superplasticity at elevated temperatures, and it has a relatively high strength at ambient temperature (~345 MPa). TTT curves for the alloy are presented, and the corresponding microstructures obtained at the various transformation temperatures are reported. Also, the results of Jominy end-quenched tests are reported and the corresponding continuous cooling kinetics are compared to the isothermal kinetics. The alloy was observed to decompose by two distinct mechanisms, depending upon the degree of supercooling. At temperatures just below the eutectoid, it decomposes into a lamellar microstructure, whereas at larger undercooling it decomposes into a coherent two-phase mixture. The interlamellar spacing and colony size are reported as a function of transformation temperature, and shown to follow expected trends. Since neither the lamellar nor coherent microstructure is superplastic, thermomechanical methods of producing a superplastic structure are discussed.

OVER the last decade many studies have been published on superplastic alloys (see Ref. 1 for a recent comprehensive review). Of major importance has been the documentation that the ability of an alloy to deform superplastically depends strongly on its microstructure.

It is well known that the microstructure of an alloy depends on its thermal and mechanical history. A common method of presenting the results of "thermal" studies is the so-called time-temperature transformation curve (isothermal). These curves record the onset of detectable transformation and the completion times of transformation on a semilog temperature *vs* time plot. When combined with the attendant microstructures, they can be useful in understanding the mechanisms and kinetics of nonisothermal transformations.

The alloy used in this study is a eutectoid Zn-Al alloy with small additions of Cu, Mg and Ca. At room temperature, the as-rolled sheet has a tensile strength of 345 MPa (50 ksi).[2] The sheet exhibits increasing superplasticity as the temperature approaches the eutectoid temperature, 278°C (551 K). The small amounts of Cu, Mg and Ca that are present in the alloy greatly reduce the kinetics of the eutectoid transformation, thereby allowing the structural aspects of the low temperature reaction to be studied in detail.[3]

The alloy exists as a solid solution α'-phase above the eutectoid temperature, 278°C (551 K). Upon cooling, the α'-phase decomposes into two-phases designated $\alpha + \beta$, where α' and α are fcc-phases with differing Zn composition and β is the hexagonal Zn rich phase. This reaction has been termed a eutectoid reaction (more properly a monotectoid reaction), and can give rise to a variety of microstructures, depending on the temperature of transformation or degree of deformation during the transformation.

FU-WEN LING is Research Metallurgist, St. Joe Minerals Corporation, Product Research and Development Department, Monaca, PA 15061 and DAVID E. LAUGHLIN is Assistant Professor, Department of Metallurgy and Materials Science, Carnegie-Mellon University, Pittsburgh, PA 15213.

Manuscript submitted September 8, 1978.

In this investigation we present the time-temperature transformation curves for the eutectoid reaction in two alloys (one has a hypereutectoid composition, 18 wt pct Al). Microstructures of the eutectoid alloys transformed through isothermal heating and continuous cooling at various cooling rates are shown. Superplastic behavior of the samples of distinct microstructures are compared and discussed.

EXPERIMENTAL PROCEDURES

A. Sample Preparation

Extruded rods and rolled sheets were used in this experiment. The rods were extruded from semicontinuously cast 1292 mm (5-7/8 in.) ingots which had been homogenized at 343°C (616 K) for 48 h and water quenched. They were extruded at 260°C (533 K) to 32 mm (1-1/4 in.) diam. The rolled sheets were rolled from semicontinuously cast billets 203 × 711 mm (8 × 28 in.) in cross-section. These billets were first homogenized at 343°C (616 K) for 48 h, breakdown rolled from 203 mm (8 in.) to 25 mm (1 in.) thick, water quenched, reheated to 260°C (533 K) and finish rolled to 2.3 mm (0.90 in.). Both these products exhibit excellent superplasticity in the temperature range 240 to 270°C (513 to 543 K).

Two different compositions of rolled sheets were used. One had the eutectoid composition (23 pct Al, 0.92 pct Cu, 0.034 pct Mg, 0.026 pct Ca, and balance Zn) and the other had a hypereutectoid composition (18 pct Al, 0.87 pct Cu, 0.037 pct Mg, 0.024 pct Ca, and balance Zn). The composition of the extruded rods was 21.2 pct Al, 0.94 pct Cu, 0.031 pct Mg, 0.012 pct Ca, and balance Zn.

B. Determination of the "TTT" Diagram

The TTT diagrams for both the eutectoid and hypereutectoid rolled sheets and the extruded rods were determined. Samples were solution heat treated at 350 ± 3°C (623 ± 3 K) for 17 to 20 h and quenched into a bath at various temperatures for various times, followed by a quench into water to room temperature. For

ISSN 0360-2133/79/0711-0921$00.75/0

temperatures greater than 100°C (373 K), an oil bath was used. For temperatures less than 100°C, a "water bath" was used for aging. The temperature fluctuation of the oil and water baths was ±1.5°C. The quench to the water bath was faster than that possible in an oil bath especially at the lower temperatures and therefore enabled the "start" time to be ascertained at temperatures below the knee of the curve. After quenching in water at room temperature, the samples were immediately examined by X-ray diffraction to determine if the reaction had commenced. The time at which the samples first exhibited a β-phase reflection was considered as the starting point of the transformation at the temperature in question. The time at which the reflection of the α'-phase completely disappeared indicated the finishing point of the transformation. The partially and completely transformed samples were also examined by optical and electron microscopy.

C. Continuous Cooling

To study the relationship of cooling rate and microstructure, Jominy tests were performed. The quenching apparatus and Jominy bars were prepared according to ASTM Specification A255-67. The bars were prepared from the extruded rods (see above).

Several small holes of 0.8 mm diam were drilled along the Jominy bar at a distance approximately 8 mm apart. A thermocouple was inserted in each hole and connected to a chart recorder so that temperature could be followed during heating and cooling of the bar. The bars were solution treated at 350°C (623 K) for two h and then immediately end-quenched until the entire bar was approximately at room temperature. The hardness values of the quenched bars were obtained after various natural aging times following quenching. The microstructures of the bar at various sections were examined using optical and electron

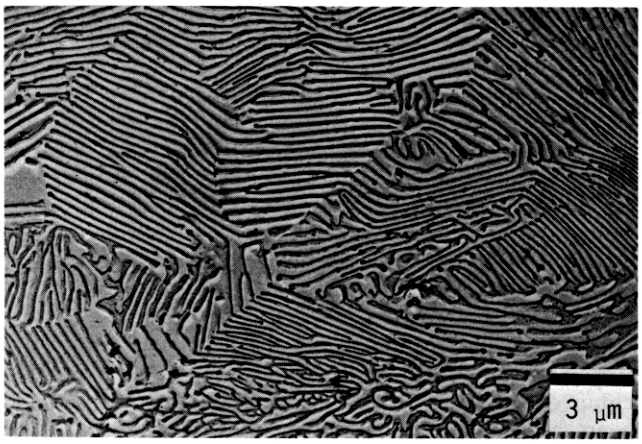

Fig. 3—Typical microstructure (TEM replica) of the 23 pct Al alloy decomposed at 265°C.

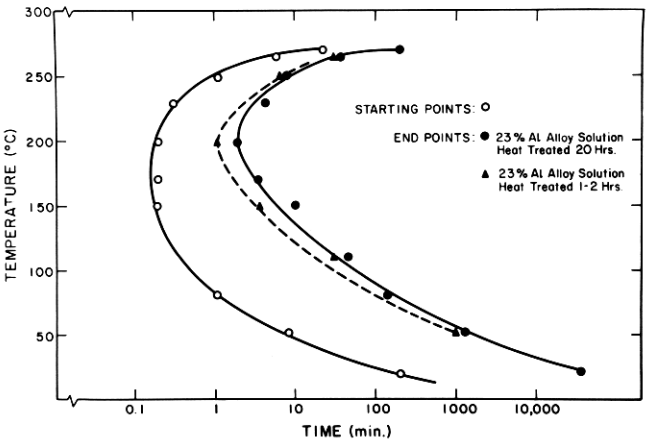

Fig. 1—TTT curves for the eutectoid transformation of 23 pct Al alloy, solution treated at 350°C.

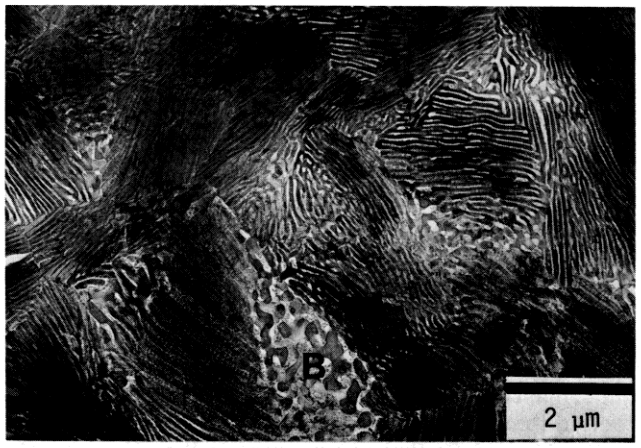

Fig. 4—TEM of the 23 pct Al alloy decomposted at 200°C.

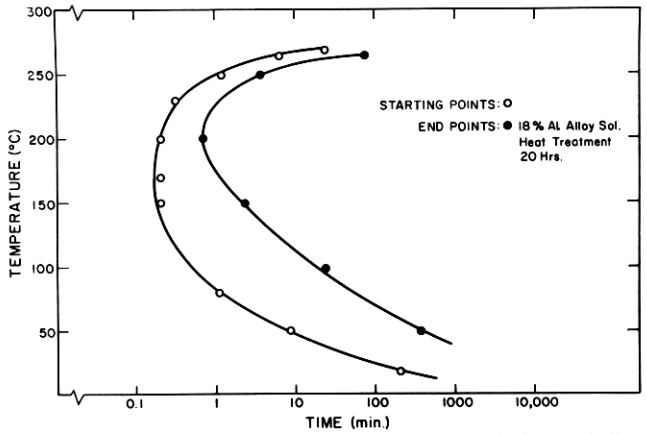

Fig. 2—TTT curves for the eutectoid transformation of 18 pct Al alloy, solution treated at 350°C.

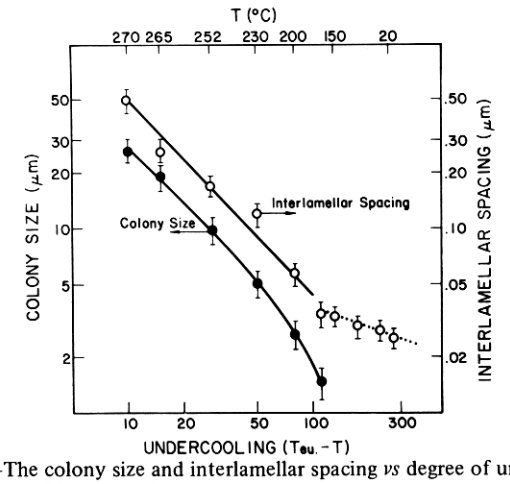

Fig. 5—The colony size and interlamellar spacing *vs* degree of undercooling, for the 23 pct Al alloy.

microscopy for the bar that had been naturally aged for four weeks.

D. Microstructure

All samples were metallographically examined, and samples with extremely fine structure were examined by replica and transmission electron microscopy (TEM). TEM was done on a JEOL-100B microscope operating at 100 kV. A double tilt stage with tilting capabilities of ±36 and ±60 deg was utilized. The interlamellar spacing and lamellar colony size were measured. Colony sizes were measured using the line intersection method. The colony which had the smallest interlamellar spacing in a photograph was chosen for the interlamellar spacing measurement. The average of three measurements from three photographs was used.

RESULTS

A. TTT Curves

The TTT curves for the eutectoid reaction:

$$\alpha' \rightarrow \alpha + \beta \qquad [1]$$

were determined as described above. Samples that were heat treated below 100°C were quenched in water instead of oil. The α'-grain size was shown to have the expected effect on the overall kinetics, *i.e.*, larger grains reduced the reaction rate. The TTT curves for the 23 pct Al alloy with grain size 21 μm (20 h at solution temperature 350°C (623 K)) and 16 μm (2 h at solution temperature) are shown in Fig. 1. At 200°C (473 K) the time for completion of the transformation in the 23 pct Al alloy varied from about one min for the smaller grain size alloy to about two min for the larger grain size (Fig. 1).

Lowering the aluminum content also has the effect of shifting the end point of transformation to shorter times (Figs. 1 and 2). For example, for the same grain size the 23 pct Al alloy completely transformed within two min at 200°C (473 K), whereas it took only 40 s to completely transform the 18 pct Al alloy. In addition to the difference in chemical driving force for transformation, this may occur because the solution temperature is not high enough to dissolve all of the β-phase. The undissolved β-phase would then act as heterogeneous sites for the reaction described in Eq. [1], thereby increasing the rate of the transformation.

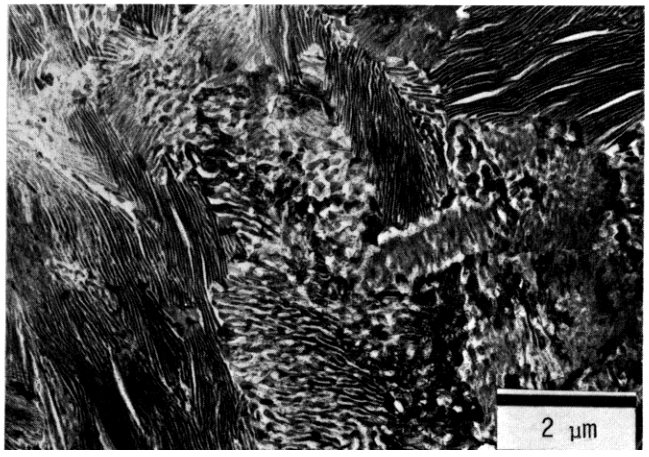

Fig. 6—TEM of the 23 pct Al alloy transformed at 150°C showing mixture of lamellar and interconnected structure.

B. Microstructure of Isothermally Heat-Treated Samples

The alloys decomposed above room temperature invariably showed partial if not complete transformation to a lamellar microstructure. At higher tem-

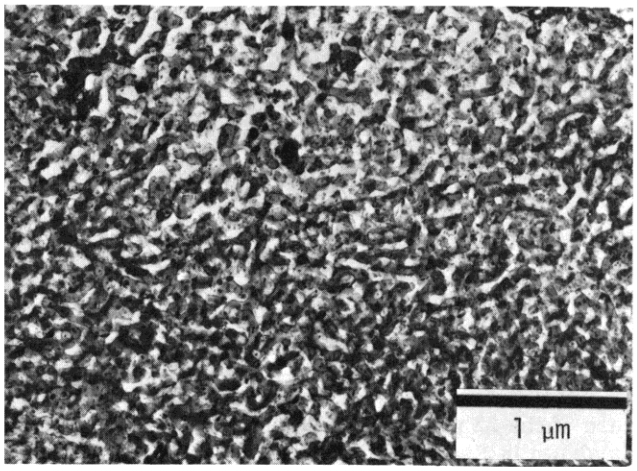

(a)

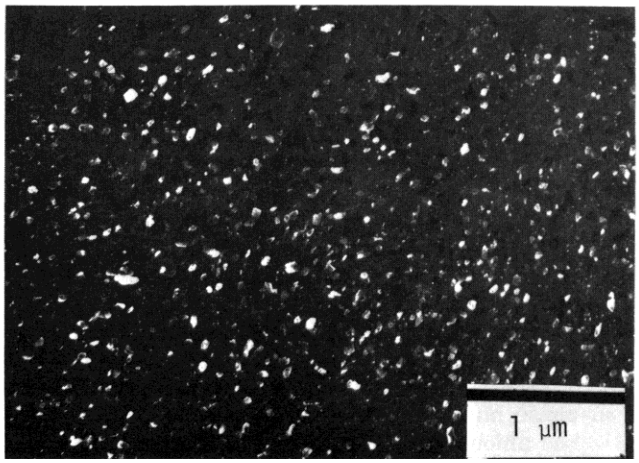

(b)

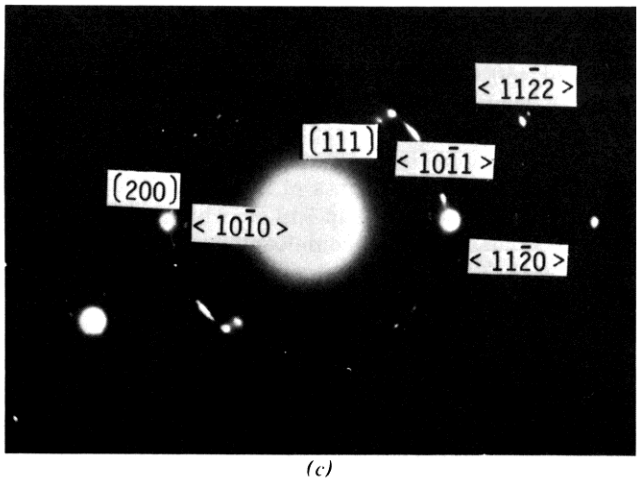

(c)

Fig. 7—TEM and SAD of the 23 pct Al alloy aged at room temperature for 21 days after quenching from 350°C: (*a*) TEM bright field, (*b*) TEM dark field from a (10$\bar{1}$1) reflection of zinc rich phase, (*c*) selected area diffraction.

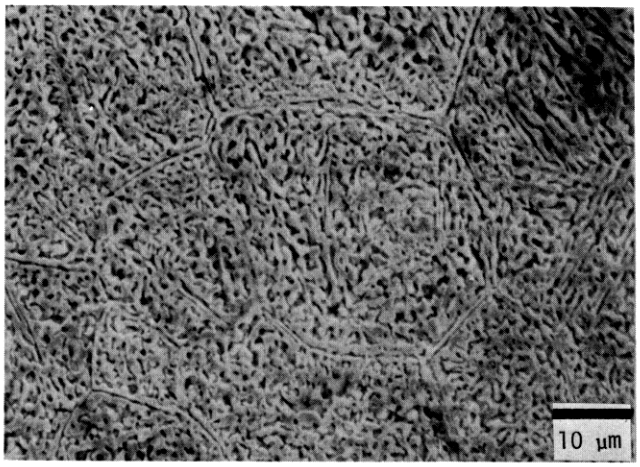

Fig. 8—Scanning electron micrograph of the 23 pct Al alloy, solution heat treated at 350°C for 20 h, water quenched and aged one day at room temperature and two days at 65°C.

peratures the interlamellar spacings were larger than at lower temperatures; the colony size also varied in a similar manner. An example of the microstructure of the 23 pct Al alloy transformed at 265°C (538 K) is shown in Fig. 3. Below about 200°C (473 K) TEM was needed to resolve the microstructure. An example of an alloy transformed at 200°C (473 K) is shown in Fig. 4. In addition to the lamellar region, this microstructure shows regions consisting of an interconnected two-phase structure. Figure 5 summarizes the lamellar spacings and colony size *vs* temperature relationship. The slope of the log of the interlamellar spacing *vs* log undercooling is seen to be approximately minus one over the temperature range 270 to 200°C (543 to 473 K) (10 to 80°C undercooling), consistent with Zener's theoretical prediction,[4] and previous experimental results for the binary Al-Zn eutectoid alloy.[5]

When isothermally heat treated at temperatures below 200°C (473 K), the samples do not completely transform to the lamellar structure as an interconnected two-phase mixture is also formed (see Fig. 4, region B). The amount of this interconnected two-phase structure increases with decreasing heat treatment temperature. For example, at 200°C (473 K) a very small amount of the interconnected microstructure is present after the completion of the reaction (Fig. 4), while at 150°C more than 30 vol pct is observed (see Fig. 6). On closer examination, this interconnected structure is seen to be made up of a single variant of α (the orientation being identical to that of the prior α'-grain) and four variants of the β-phase. This is shown by TEM and SAD in Fig. 7, which is from a sample transformed at room temperature. Also shown is a dark-field electron micrograph of one of the β-variants. By SAD it was determined that four variants of the β-phase were present, implying that the orientation relationship between β and α was:

$$(0002)_\beta \parallel \{111\}_\alpha$$

Since these planes are similar in atomic arrangement and interatomic spacing, it seems likely that the β-phase has formed coherently with the α. A SEM micrograph of an etched sample is shown in Fig. 8, to indicate more clearly the interconnectivity of the two-phases. This interconnected microstructure will be termed the "coherent microstructure."

These two transformation microstructures (coherent and lamellar) occur by distinct mechanisms. The mechanisms yielding the lamellar microstructure starts at the grain boundaries and inclusions (heterogeneous), while the "coherent" transformation occurs throughout entire grains (*i.e.*, homogeneously). Figure 9 shows an optical micrograph of the 23 pct Al alloy that has been partially transformed at 150°C for one min and water quenched. The lamellar structure can be seen to form at the prior α'-boundaries. After the quench, the coherent microstructure forms in the grain interior by a homogeneous mechanism.

C. Jominy Bar End Quenching

1. Jominy Hardness Curves. Three Jominy bars were separately solution treated at 350°C (623 K) for two h and end quenched. Hardness values along the bars were tested within one h after quenching and, as seen in Fig. 10, good reproducibility was obtained. The change in hardness along the bar can be explained by transformation phenomenon. In contrast to the Jominy bars of steels, the quenched end of this alloy has a low hardness value because it consists of the

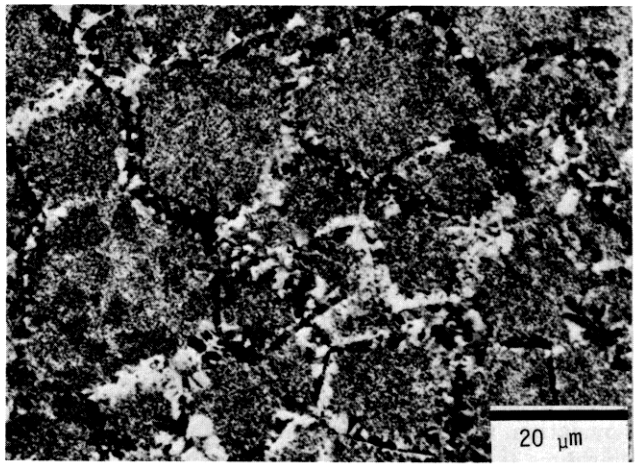

Fig. 9—Optical micrograph using polarized light of the 23 pct Al alloy isothermally decomposed at 150°C for one min. Transformation started at the prior α'-grain boundaries.

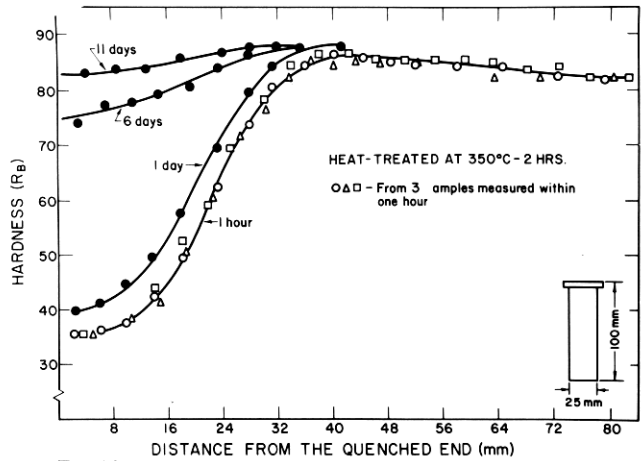

Fig. 10—Hardness curves of the end-quenched Jominy bar.

retained solid solution α'-phase. As the distance from the quenched end increases, the hardness increases to a maximum. This corresponds to the complete transformation of α'-phase to a fine lamellar structure. Beyond this maximum, a decrease in hardness values occurs because of the increase in interlamellar spacing (see Fig. 5). Also, the decrease in the amount of zinc in solid solution in the aluminum rich phase (because of the decrease in cooling rate) would contribute to this slight decrease in hardness.

The changes in the hardness curve with aging times measured on a single sample are also shown in Fig. 10. The hardness values at the quench-end increase with aging time up to 11 days of aging; after that, no significant change in hardness is seen, indicating that the transformation is complete. The transformation at room temperature gives rise to the coherent microstructure.

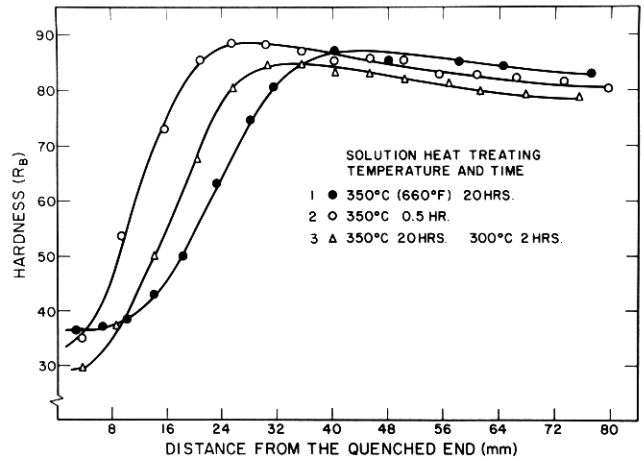

Fig. 11—Hardness curves of the Jominy bar quenched from various solution heat treating conditions.

2. Jominy Hardness Curves *vs* α'-Grain Size and Temperature Prior to the Quenching. Two samples with different α' grain sizes were prepared by heat treating at 350°C (623 K) for 20 h and 0.5 h. The α'-grain sizes are approximately 14 and 11 μm, respectively. The hardness curves of these two samples, immediately after end quenching, are shown in Fig. 11. Just as in isothermal heat treatment, the sample with the smaller α'-grain size transforms faster, *i.e.*, the nontransformed portion of the bar indicated by lower hardness values is seen to be less in extent. The temperature immediately prior to quenching also has an effect on the hardness curve, shown by curve 3 of Fig. 11. For the same α'-grain size, the sample quenched from a lower temperature has a less extensive nontransformed section as well as a lower hardness value at the completely untransformed end.

3. Cooling Curves and TTT Diagram. The measured cooling curves at various positions on the Jominy bar are shown in Fig. 12. The eutectoid decomposition, which occurs during cooling, generates heat and changes the cooling rate (seen most clearly in the upper curve). Therefore, the start of the transformation during cooling is revealed by the change in slope of the cooling curve. It is interesting to note

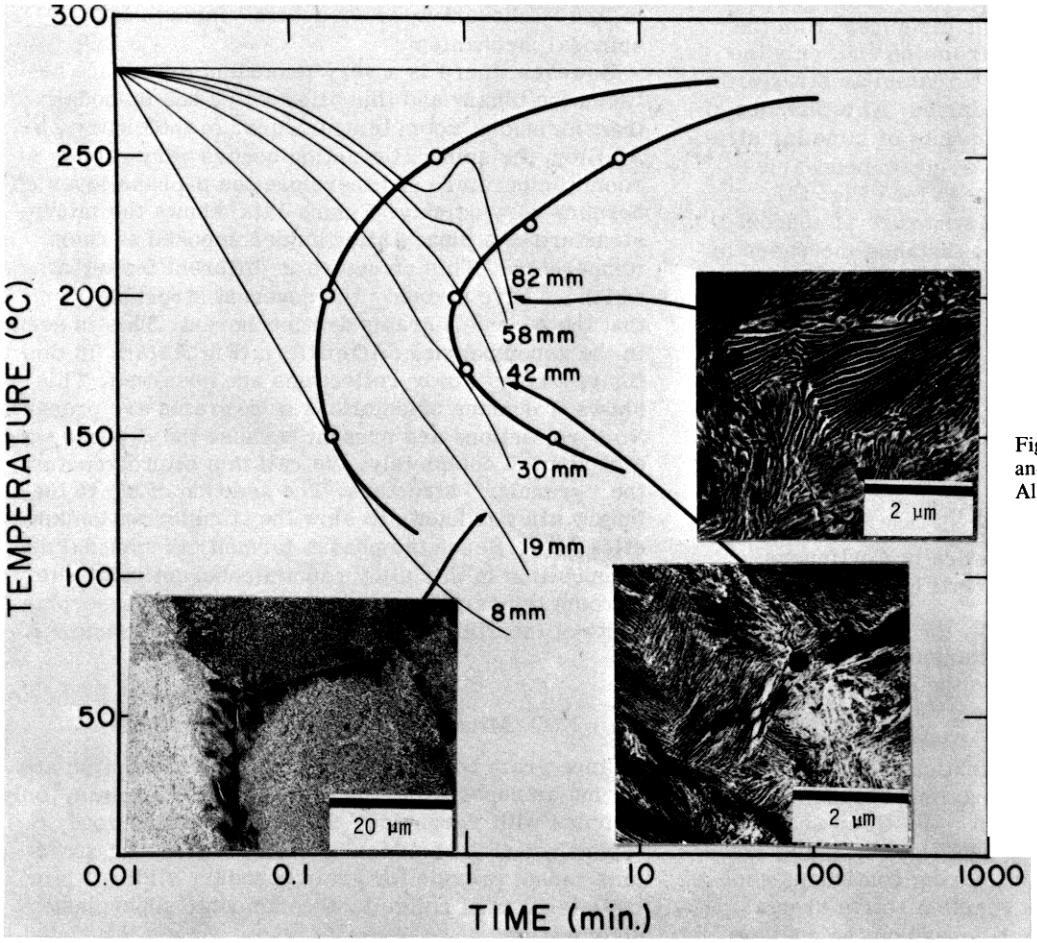

Fig. 12—TTT curves, cooling curves and microstructures of the 23 pct Al alloy.

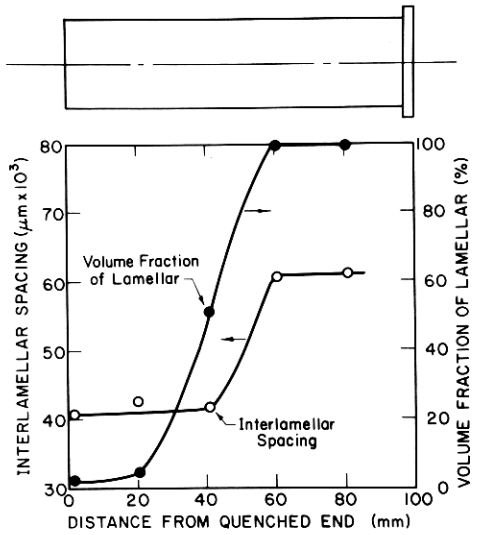

Fig. 13—Interlamellar spacing and volume fraction of lamellar along the end-quenched Jominy bar.

that transformation starts at approximately the same time, ~35 s, independent of the cooling rate.

The TTT curves determined by X-ray diffraction using the same extruded sample are also shown in Fig. 12. The difference in transformation kinetics of the sample under isothermal heating and continuous cooling is clearly observed.

4. Microstructure. The end-quenched sample was sectioned and examined by transmission electron microscopy one month after quenching. The foils for electron microscopy were taken approximately at the center of the bar and at various distances from the quenched end. Within 10 mm from the end, only the coherent structure was seen. No lamellar structure was seen at the α'-grain boundaries. At a distance of 19 mm from the end, small amounts of lamellar structure nucleated and grew from α'-grain boundaries and other defect sites can be seen (see Fig. 12).

At 42 mm from the end, the structure is approximately 80 pct lamellar. As the distance increases to 58 mm, only the lamellar structure is present and the interlamellar spacing is much larger than that at 42 mm from the end (see Fig. 12). The interlamellar spacing is approximately the same at 58 and 82 mm from the end. The changes in volume fraction and interlamellar spacing with distance from the quenched end are shown in Fig. 13.

DISCUSSION

A. Transformation Kinetics in Continuous Cooling *vs* Isothermal Heating

In isothermal heat treatment, the maximum transformation rate occurs at an intermediate temperature. At temperatures close to the eutectoid, the atomic mobility is high but the driving force for the transformation is small. At low temperatures, the driving force for the transformation is high but the atomic mobility is low. The maximum transformation kinetics for the alloy occurs at ~185°C, as shown at the nose of the TTT curves (see Figs. 1, 2, and 12).

In the reaction that occurs during continuous cooling, it is observed that the reaction starts over a range of temperatures which depend on the cooling rates (see Fig. 12). However, the "start" times are observed to occur at approximately the same time (about 35 s) for each of the cooling rates. This can be understood in terms of the shape of the TTT curve and the well-known "shift to the right" of continuous transformation curves with respect to their corresponding isothermal transformation curve. If the TTT curve, shown in Fig. 12, is shifted to the right, it is apparent that the "start" time will be approximately the same over a large range of temperatures. This "shift" in the knee changes its position by a factor of about three, which is commensurate with the shift in other published continuous cooling curves.[6]

B. Transformation Mechanism

Nuttall and Nicholson[7] and Ardell, Nuttall and Nicholson[8] have interpreted the room temperature reaction in the binary eutectoid alloy as occurring by the spinodal mechanism. For an elastically isotropic matrix, this mechanism predicts the formation of a two-phase interconnected microstructure, with specific orientation relations between the phases.[9] If this alloy were to initially decompose spinodally, the zinc enriched regions could transform to the β-phase. It would be expected that the (0002) basal planes of the zinc phase would be parallel to the {111} planes of the fcc aluminum rich matrix. This expected orientation relationship and the interconnected structure is identical to that observed here in this alloy (see Figs. 7 and 8). Hence our results agree with Nuttall and Nicholson's interpretation of the results on the binary alloy. That is, the "coherent microstructure" forms *via* the spinodal mechanism.

However, there is a very important difference between the binary and this alloy which has spinodally transformed at room temperature. In the binary Zn-Al alloy, the spinodal reaction occurs very rapidly at room temperature and therefore the β-phase loses coherency very quickly. Figure 14(*a*) shows the microstructure of a binary alloy as decomposed at room temperature. This structure is different from that which we have termed "the coherent structure," in that the α- and β-grains are incoherent. This is seen in the accompanying SAD pattern (Fig. 14(*b*)). In this figure "rings" of α-reflections are observed. This shows that many orientations of α-grains are present. No β-reflections are present because the β-phase was etched away completely. We call this microstructure the "granular" structure. The addition of Mg to the binary alloy is known to slow the transformation kinetics.[3,10,11] Hence the phases formed *via* spinodal decomposition in this alloy remain coherent indefinitely at room temperature. How this affects the superplasticity of the alloy is the topic of the next section.

C. Microstructure and Superplasticity

Since grain boundary sliding and grain rotation are the major superplastic deformation mechanisms,[1] only samples with "granular" structure possess good superplasticity. A material having a coherent structure cannot provide for grain boundary sliding while lamellae cannot rotate to accommodate superplastic deformation.

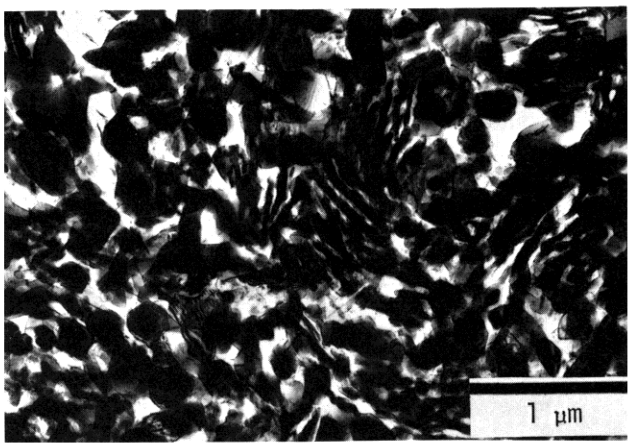

(a)

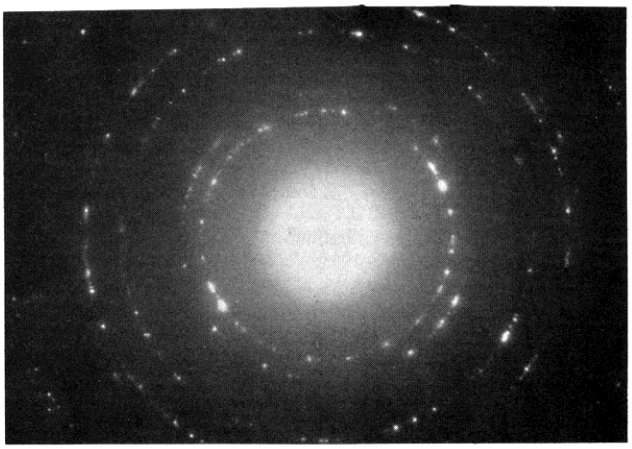

(b)

Fig. 14—TEM and SAD of a binary Zn-Al eutectoid alloy solution heat treated at 350°C and water quenched.

To illustrate that only the "granular" microstructure exhibits good superplasticity, three tensile specimens with different microstructures were prepared and tested: one with a granular, one with a lamellar and one with a coherent microstructure. The granular specimen was prepared from the as-extruded rod; the lamellar specimen was produced by holding the as-extruded rod at 350°C (623 K) for 2 h and subsequently cooling in air, while the coherent sample was prepared by holding the as-extruded rod at 350°C (623 K) for 2 h followed by a water quench. Figure 15 shows these three tensile specimens after being tested at 260°C (533 K) to 300 pct elongation.

Because of their respective microstructures, the specimens with the lamellar and coherent microstructure exhibit necking early in the deformation process. However, the extensive deformation in the necked regions, in combination with the elevated temperature during the deformation process, changes each of the specimens' microstructure to the granular one (see Fig. 15, and compare the microstructure before and after deformation). Thereafter, both specimens deform superplastically. The specimens with the granular microstructure deformed superplastically from the start of the deformation process.

It is evident that if the alloy under investigation is to be superplastic it must have the granular microstructure. To obtain this microstructure samples with either the lamellar or coherent one must be mechanically deformed at elevated temperatures. This is in contrast to the binary Zn-Al alloy in which excellent superplasticity may be obtained in specimens that are transformed after quenching from the α'-phase[12] (*viz* after spinodal decomposition). As mentioned previously this is because the spinodal reaction and subsequent coarsening occurs quite rapidly in the

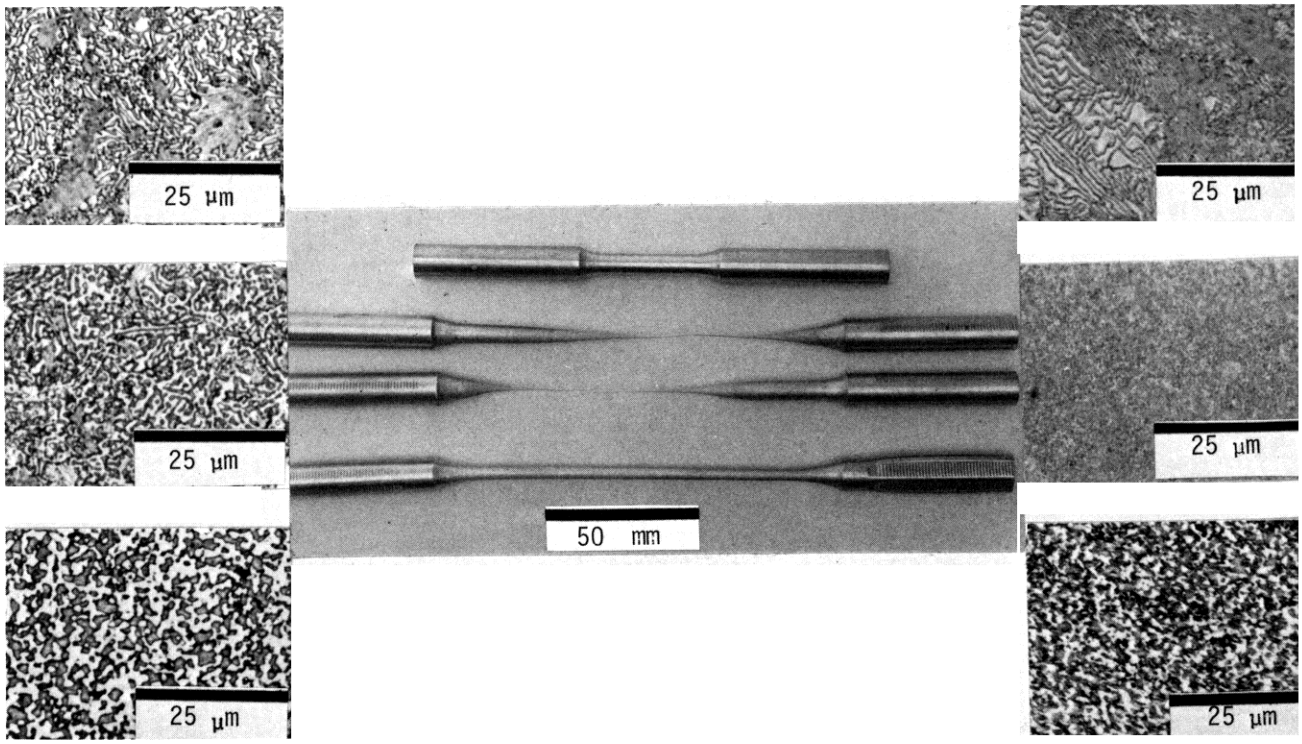

Fig. 15—Elevated temperature tensile behavior of the samples with various microstructures. Microstructure of the samples prior to tensile test shown on the right; after tensile testing shown on the left.

binary alloy, giving rise to an incoherent fine mixture of equiaxed $\alpha + \beta$-grains. In the present alloy deformation must be applied to break up the coherent $\alpha + \beta$-mixture into the granular incoherent mixture of the $\alpha + \beta$-phases.[2]

SUMMARY AND CONCLUSIONS

1) The isothermal time-temperature transformation curves for two commercial Zn-Al alloys that exhibit superplasticity have been determined, and compared with their continuous cooling kinetics.

2) Alloys decomposing above the knee of the transformation curve exhibit lamellar microstructures. The log of the interlamellar spacing is proportional to the log of $1/\Delta T$. The alloy with this structure does not exhibit superplasticity.

3) Alloys decomposing below the knee of the transformation curve exhibit mostly coherent microstructure. The coherent structure remains coherent at room temperature for indefinite times. The alloy with this structure does not possess superplasticity either.

4) In this alloy, the coherent structure can only be transformed to an incoherent one by elevated temperatures mechanical processing, *i.e.*, thermomechanical treatment. Alloys produced by this process exhibit good superplasticity between 240 to 270°C (513 to 543 K).

ACKNOWLEDGMENTS

The authors would like to thank S. C. Chang for the X-ray diffraction work, R. W. Balliett for his valuable suggestions during the investigation, and P. H. Abramowitz for his helpful criticism and discussion. Also L. A. Nesbit and R. J. Rioja are thanked for their assistance with the TEM work, and Mr. D. R. Forse for assistance with the Jominy testing.

The permission for publication by the management of St. Joe Minerals Corporation is gratefully appreciated.

Support from the Materials Research Laboratory Section, Division of Materials Research, National Science Foundation through use of central research facilities is also gratefully acknowledged.

REFERENCES

1. J. W. Edington, K. N. Melton, and C. P. Cutler: *Progr. Mater. Sci.*, 1976, vol. 21, pp. 61-170.
2. Fu-Wen Ling: *Proc. of Symp. on Thermomechanical Processing of Aluminum Alloys*, AIME, in press, 1978.
3. T. L. Bartel and K. B. Rundman: *Met. Trans. A*, 1975, vol. 6A, p. 1887.
4. C. Zener: *Trans. AIME*, 1946, vol. 167, p. 550.
5. D. Cheetham and N. Ridley: *J. Inst. Metals*, 1971, vol. 99, p. 371.
6. *Atlas of Isothermal Transformation and Cooling Transformation Diagrams*, ASM, Metals Park, OH, 1977.
7. K. Nuttall and R. B. Nicholson: *Phil. Mag.*, 1968, vol. 17, p. 1087.
8. A. J. Ardell, K. Nuttall, and R. B. Nichols: *The Mechanism of Phase Transformations in Crystalline Solids*, Institute of Metals, 1969.
9. J. W. Cahn: *Trans. TMS-AIME*, 1968, vol. 242, p. 166.
10. A. J. Perry: *Acta Met.*, 1966, vol. 14, p. 1143.
11. M. Murakami, O. Kawano, and Y. Murakami: *Trans. TMS-AIME*, 1969, vol. 245, p. 815.
12. R. H. Johnson, C. M. Packer, L. Anderson, and O. D. Sherby: *Phil. Mag.*, 1968, vol. 18, p. 1309.